



HAL
open science

Determination of the degree of hydration of Portland cement using three different approaches: Scanning electron microscopy (SEM-BSE) and Thermogravimetric analysis (TGA)

Duc Chinh Chu, Joelle Kleib, Mouhamadou Amar, Mahfoud Benzerzour,
Nor-Edine Abriak

► To cite this version:

Duc Chinh Chu, Joelle Kleib, Mouhamadou Amar, Mahfoud Benzerzour, Nor-Edine Abriak. Determination of the degree of hydration of Portland cement using three different approaches: Scanning electron microscopy (SEM-BSE) and Thermogravimetric analysis (TGA). *Case Studies in Construction Materials*, 2021, 15, pp.e00754. 10.1016/j.cscm.2021.e00754 . hal-03770251

HAL Id: hal-03770251

<https://hal.science/hal-03770251v1>

Submitted on 5 Jan 2024

HAL is a multi-disciplinary open access archive for the deposit and dissemination of scientific research documents, whether they are published or not. The documents may come from teaching and research institutions in France or abroad, or from public or private research centers.

L'archive ouverte pluridisciplinaire **HAL**, est destinée au dépôt et à la diffusion de documents scientifiques de niveau recherche, publiés ou non, émanant des établissements d'enseignement et de recherche français ou étrangers, des laboratoires publics ou privés.



Distributed under a Creative Commons Attribution - NonCommercial 4.0 International License

1 **Determination of the degree of hydration of Portland cement using three different approaches:**
2 **Scanning electron microscopy (SEM-BSE) and Thermogravimetric analysis (TGA)**

3 **Duc Chinh CHU⁽¹⁾, Joelle KLEIB⁽¹⁾, Mouhamadou AMAR⁽¹⁾, Mahfoud BENZERZOUR⁽¹⁾, Nor-Edine**
4 **ABRIAK⁽¹⁾**

5 ⁽¹⁾ Univ.Lille, IMT Lille Douai, Univ.Artois, Yncrea Hauts-de-France, ULR 4515-LGCgE, 6 Laboratoire de Génie
6 civil et géo-Environnement, F-59000, Lille, France

7
8 (*) Corresponding author: Duc Chinh CHU

9 Email: duc.chinh.chu@imt-lille-douai.fr

10 Univ.Lille, IMT Lille Douai, Univ.Artois, Yncrea Hauts-de-France, ULR 4515-LGCgE, 6 Laboratoire de Génie
11 civil et géo-Environnement, F-59000, Lille, France

12
13 **Abstract**

14 Cement paste hydration is a complex physical-chemical process. The aim of this paper is to use three approaches to
15 determine the degree of hydration: portlandite quantification, scanning electron microscopy and bound water
16 quantification. In order to investigate the physical-chemical and mechanical properties, as well as the hydrates
17 generated. Portland cement was synthesized and characterized in the laboratory. At all hydration durations, the
18 portlandite quantification method and SEM-BSE image analysis show similar results. The method of SEM images
19 analysis requires time to gather and process images, but is unaffected by the type of hydrates produced. The bound
20 water quantification method gives a lower degree of hydration than two other methods at all hydration times. To test
21 the reliability of these procedures, the compressive strength was calculated based on the degree of hydration. The
22 results indicate that the portlandite quantification method and SEM-BSE image analysis are more accurate than the
23 bound water quantification approach in terms of reproducing the experimental results.

24
25 **Keywords:** Cement, Hydration, Portlandite, Bound water, SEM-BSE, Compressive strength.

62
63
64

I. Introduction

65 Portland cement is a mixture of clinker and calcium sulfate in a ratio of approximately 95:5% [1]. Cement is one
66 of the essential constituents in the manufacture of concrete; the most widely used building material in the world. The
67 mineralogical composition of clinker consists of alite (C_3S : Ca_3SiO_5), belite (C_2S : Ca_2SiO_4), tricalcium aluminate
68 (C_3A : $Ca_3Al_2O_6$) and tetra-calcium aluminoferrite (C_4AF : $Ca_4Al_2O_{10}Fe_2$). During hydration, the cement reacts with
69 water resulting in the formation of different hydrates. Ettringite is formed from the reaction of calcium sulfate,
70 tricalcium aluminate and water. The reaction of the silicates leads to the formation of portlandite (CH) and a
71 Calcium Silicate Hydrate (C-S-H).

72 Previous studies [2, 3] have shown that C-S-H is the main hydrate of hydrated cement paste and contributes
73 significantly to macro-properties of concrete such as strength and durability.

74 The composition of the C-S-H, depends on the water to cement ratio (w/c ratio), the temperature as well as the
75 composition of the cement [4–6]. Indeed, in the literature, there are three distinct phases C-S-H depending on the
76 C/S (CaO/SiO_2) ratio:

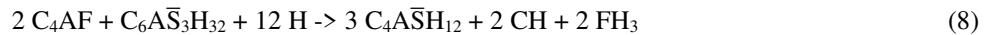
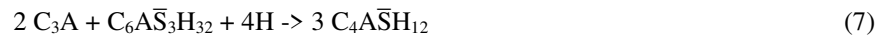
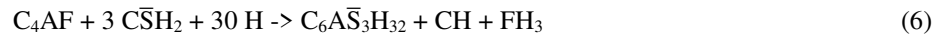
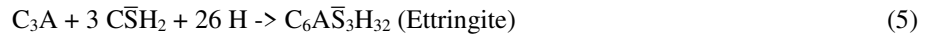
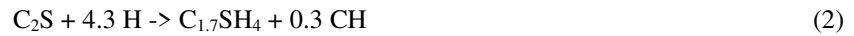
- 77 • C-S-H (α): $0.66 < C/S < 1$ formed when the $[Ca^{2+}]$ concentration is less than 2 mmol/l.
- 78 • C-S-H (β): $1 < C/S < 1.5$ formed when the $[Ca^{2+}]$ concentration is between 2 and 22 mmol/l.
- 79 • C-S-H (γ): $C/S = 1.7$ formed when the $[Ca^{2+}]$ concentration is greater than 22 mmol/l.

80 In addition, Phung et al [7] have shown that the C/S molar ratio of the cement paste was critical in determining
81 the microstructure of C-S-H and the decrease in the C/S ratio can alter the microstructure of C-S-H.

82 The amount of hydrates formed during hydration depends on the degree of hydration which is defined as a ratio
83 of the amount of hydrated cement to that of the initial anhydrous cement. There are several experimental approaches
84 to determine the degree of hydration of cement such as:

- 85 • Scanning electron microscopy (SEM-BSE) [8, 9].
- 86 • X-ray diffraction (XRD) [10].
- 87 • Thermogravimetric analysis (TGA) [11].
- 88 • Measurement of the heat of hydration by isothermal calorimetry [9, 12].
- 89 • Nuclear magnetic resonance (NMR) [3, 13].
- 90 • Compressive strength [14].

91 Several studies have employed the thermal analysis method (TGA) to determine the degree of hydration of
92 cement. The basic idea is to use the following simplified equations ((Eq1) -> (Eq8)) to measure the portlandite
93 amount (CH) [10, 11] and chemically bound water [12] generated during hydration [15–17].



94 In a recent study, Lei et al [3] used the $Ca(OH)_2$ quantification method measured by TGA analysis and the NMR
95 method for the determination of the degree of hydration of cement paste ($W/C = 0.3$). The ^{29}Si NMR and ^{27}Al NMR
96 is used to quantify the phases containing these element in a cementitious material. Good consistency between the
97 two methods was observed (74.0% for the $Ca(OH)_2$ quantification method at 28 days and 78.4% for the NMR
98 method at 28 days). However, in his study, the degree of hydration was calculated according to the equation (Eq9):

$$\alpha(t) = \frac{m_{Ca(OH)_2}}{25 \text{ wt.}\%} * 100 \quad (9)$$

99 Knowing that the 25% value is not always constant because the mineral composition of cement is always
100 variable. In addition, the NMR method is a complicated method (long analysis time, 1 day for ^{29}Si NMR analysis),
101 therefore, in this study, three methods used are: Method 1: Portlandite quantification method, Method 2: Bound
102 water of quantification method, Method 3: SEM-BSE image analysis method.

103 The first approach for evaluating the degree of hydration is to use the following equations to calculate the
104 $Ca(OH)_2$ amount estimated from the TGA analysis according to (Eq10):

$$m_{Ca(OH)_2} = \frac{\Delta m_{450^\circ C - 550^\circ C(t)} \cdot M_{Ca(OH)_2}}{M_{H_2O}} \quad (10)$$

105 with:

106 $m_{Ca(OH)_2}$: Amount of $Ca(OH)_2$.

107 $\Delta m_{450^\circ C - 550^\circ C(t)}$: The mass loss of the samples between $450^\circ C$ and $550^\circ C$ from the TGA analysis.

108 $M_{Ca(OH)_2}$: Molar mass of $Ca(OH)_2$ equal to 74.09 g/mol .

109 M_{H_2O} : Molar mass of water equal to 18 g/mol .

110 Then the degree of hydration of the cement can be calculated using the equation below (Eq11):

$$\alpha(t) = \frac{m_{Ca(OH)_2}}{m_c \cdot 0} \quad (11)$$

The mass of the sample can be calculated using the equation (Eq12):

$$m_c = \frac{m_{sample}}{\left(1 + \frac{w}{c}\right) \cdot (1 + LOI)} \quad (12)$$

111 with:

112 $\alpha(t)$: Degree of hydration of the cement at time t .

113 m_{sample} : Mass of the samples.

114 m_c : Mass of the initial cement.

115 Y_0 : Amount of $Ca(OH)_2$ produced upon complete hydration of the cement. This value depends on the composition of the cement as well as the stoichiometry of the C-S-H gel of the cement hydration reactions (Eq(1) -> Eq(8)).

116 w/c : the water to cement ratio of the paste.

117 LOI: loss of cement on ignition.

118 The second experimental approach for determining the degree of hydration of cement recommended by the
120 National Institute of Standards and Technology (NIST) consists in determining the amount of water chemically
121 bound according to the following equation (Eq13):

$$\alpha(t) = \frac{W_n(t)}{W_n(\infty)} * 100 \quad (13)$$

122 with:

123 $\alpha(t)$: degree of hydration of the sample at time t .

124 $W_n(t)$: amount of bound water for a sample at time (in gram of water per 100 g of anhydrous cement).

125 $W_n(\infty)$: amount of water bound for a completely hydrated sample (in gram of water per 100 g of anhydrous
126 cement).

127 The $W_n(t)$ value can be determined experimentally by (Eq14) if the two following conditions are met:

- 128 • No carbonation in the cement paste.
- 129 • Low weight loss of anhydrous cement before $1000^\circ C$

$$W_n(t) = \frac{\Delta m_{sample(105^\circ C - 1000^\circ C)(t)}}{m_{sample(1000^\circ C)(t)}} * 100 \quad (14)$$

130 In order to determine the $W_n(\infty)$ value, NIST provides an approximate theoretical estimation of the amount of
131 bound water produced for the five main mineral phases of cement after hydration is complete [18].

132 The third method consists of the SEM-BSE image analysis technique to study the distribution of phases in the
133 observation area. Indeed, this technique has been frequently applied to examine the cementitious material's
134 microstructure [19]. In an SEM-BSE image, the backscatter coefficient increases monotonically with the average
135 atomic number of each phase [20]. This allows differentiating and quantifying of each crystalline phases in the
136 analysis area. However, in cement-based materials, the backscattering coefficients of numerous hydration products
137 (C-S-H, Ettringite, etc.) are too similar to be separated individually on the histogram [19]. Because the epoxy
138 backscatter coefficient is substantially lower than the other phases, the pores may be easier to segment [19].

139 The SEM-BSE image analysis has been used to quantify phases of hydrated cement paste [21], to study the
140 phase distribution in the mortar interphase zone [22], and to estimate the reaction fraction of mineral additions in the
141 cement matrix [9]. The three steps in this approach are as follows:

- 142 • Choice of magnification and resolution of the image.
- 143 • Phase segmentation by gray level thresholds.
- 144 • Quantification of phases in the analysis area.

145 Table 1 summarizes the advantages and disadvantages of the three methods of determining the degree of
146 hydration used in this study.

147 Table 1

148 Advantages and disadvantages of the three methods (Method 1: $Ca(OH)_2$ quantification method, Method 2: Bound
149 water of quantification method, Method 3: SEM-BSE image analysis method).

Method	Method 1	Method 2	Method 3
--------	----------	----------	----------

Advantages	<ul style="list-style-type: none"> Ease of sample preparation. Ease of processing the result. 	<ul style="list-style-type: none"> Ease of sample preparation. Ease of processing the result. 	<ul style="list-style-type: none"> Apply cement containing a pozzolanic mineral addition, a slag.
Disadvantages	<ul style="list-style-type: none"> Do not apply cement containing a pozzolanic mineral addition. 	<ul style="list-style-type: none"> An adequate analysis program to avoid the loss of bound water. 	<ul style="list-style-type: none"> Difficulty of sample preparation Difficulty of processing the result.

150 There have been no researches published to far that compare the various methods for determining the degree of
151 hydration of CEM I cement. Therefore, the purpose of this study is to compare the feasibility and reliability of the
152 SEM –BSE image analysis approach for estimating the degree of hydration of cement with two other methods using
153 the thermogravimetric analysis (TGA).

154 II. Material and method

155 II.1. Method of characterization of the synthesized clinker and cement

156 The clinker cement (OPC 97TM) used in this study was synthesized in the laboratory by burning a mixture of
157 limestone (CaCO₃), silica oxide (SiO₂), aluminum oxide (Al₂O₃) and iron oxide (Fe₂O₃). The proportion of
158 components was calculated using the modulus usually used in the cement industry: the Lime Saturation Factor
159 (LSF), the Silica Ratio (SR) and the Alumina Ratio (AR). The calculations of modulus (LSF, SR and AR) are
160 presented by the equations below ((Eq15) -> (Eq17)):

$$LSF = \frac{100 * \%CaO}{2.8 * \%SiO_2 + 1.18 * \%Al_2O_3 + 0.65 * \%Fe_2O_3} \quad (15)$$

$$SR = \frac{\%SiO_2}{\%Al_2O_3 + \%Fe_2O_3} \quad (16)$$

$$AR = \frac{\%Al_2O_3}{\%Fe_2O_3} \quad (17)$$

161 In this study, the values LSF = 97, SR = 2.6 and AR = 1.45 were used for the formulation of mixture. Table 2
162 shows the composition of the components of the formulation.

163 **Table 2**
164 Mix design for the production of the clinker cement OPC 97TM.

Formula	Limestone (wt. %)	Alumina oxide (wt. %)	Iron oxide (wt. %)	Silica oxide (wt. %)
OPC 97TM	79.99	3.17	2.32	14.52

165 The raw materials were first mixed by adding water with a water/material ratio = 0.6 in order to have good
166 homogeneity. After drying at 105°C, pellets (with a diameter of 40 mm and a height of 15 mm) are formed using a
167 press and a force of 5 KN. The pellets were burned in a furnace at 200°C for 20 minutes, then the temperature
168 increases to 1450°C with a heating rate of 7°C/minute, and kept at this temperature for 15 minutes. After
169 clinkerization, the obtained clinkers were cooled in the furnace to reach the room temperature. Portland cement was
170 produced by adding gypsum (CaSO₄.2H₂O) to ground clinker in order to have an SO₃/Al₂O₃ molar ratio of 0.6.

171 The content of free lime in the clinker was determined by the Schlafer-Bukokowski method. Indeed, cement
172 manufacturers consider that a clinker, whose composition is perfectly dosed, has a CaO_{free} content of less than 2%
173 wt. [23]. Therefore, in this study, the maximum acceptable CaO_{free} content is set at 2%.

174 The mineralogical composition of the clinker was identified by X-ray diffraction (XRD) and quantified
175 according to the Bogue modified formula, which takes into account the presence of CaO_{free} [24].

176 The chemical composition of the clinker and hydrated cement paste phases was analyzed on the polished
177 sections using a Hitachi S-4300 SE/N scanning electron microscope operating in backscattered electron mode (20
178 keV) and equipped with an energy dispersive X-ray spectrometer (EDS). For the measurement, the points were
179 carried out on several zones.

180 The particle size distribution of the OPC 97TM cement was measured using the Beckman Coulter – LS13 320
181 type device after dispersing in an ethanol solution. The absolute density of the OPC 97TM cement was carried out

182 using an Accupyc 1330 helium pycnometer. The Blaine specific surface of the cement was measured according to
 183 standard NF EN 196-6 [25]. In this study, the Blaine surface of the cement is between 3500 and 4000 cm²/g.

184 The chemical composition of the synthesized cement was verified by X-Ray fluorescence (XRF). The
 185 mineralogy of cement and hydrated cement paste was analyzed by X-ray diffraction (XRD) using a BRUKER D2
 186 Advance device equipped with a Cu anticathode, $\lambda = 1.5406 \text{ \AA}$ with the angle 2θ from 5° to 80° and a step of 0.02.

187 II.2. Method for determining the degree of hydration

188 In this study a cement pastes with a w/c ratio of 0.5 was used to determine the degree of hydration. After three
 189 minutes of mixing, the paste was introduced into the polytetrafluethylene molds for measuring the degree of
 190 hydration, and into the 1x1x1 cm³ size molds for the measurement of compressive strength. The cement pastes were
 191 demolded after 24 hours and stored in the saturated lime solution.

192 Based on previous studies [23, 26–29], the compressive strength of the cement paste was measured on the cube
 193 of dimension 1x1x1 cm³ under a constant stress of 0.3 MPa/s using a uniaxial press at 2, 15 and 28 days of
 194 hydration. For each measurement, 6 samples were tested.

195 II.2.1. Determination of the degree of hydration by thermogravimetric analysis (TGA)

196 To prevent carbonation of the cement paste, in this study, no method of stopping hydration was used. The
 197 cement paste for the TGA analysis was analyzed immediately upon reaching the desired hydration time. The device
 198 used is the NETZSCH STA 409 type with the following experimental conditions:

- 199 • During the analysis the sample is kept under a flow of Argon at a flow rate of 75 ml/min.
- 200 • The temperature increases from 30 °C to 105 °C at a rate of 2 °C/min, then maintained at 105 °C for 1 hour
 201 before increasing to 1100 °C at a rate of 3 °C/min.

202 II.2.2. Determination of the degree of hydration by the SEM-BSE image analysis method

203 To stop the hydration, the samples for image analysis were submerged in an acetone solvent solution. Indeed,
 204 drying samples at 105 °C has the potential to alter the microstructure of the cement paste [30] and so impair image
 205 analysis results. A JEOL scanning electron microscope operating in backscattered electron mode (15 keV) with a
 206 magnification of 500 and a resolution of 1280 x 960 pixels was used to capture images of the sample. For the
 207 measurement, around 20 pictures were taken at various positions throughout the sample.

208 III. Results

209 This part presents, on the one hand, the result of characterization of the cement (OPC 97TM) and the cement
 210 paste in order to assess the quality of the cement synthesized in the laboratory, and on the other hand, the results of
 211 the degree of hydration of the paste determined by three different methods.

212 III.1. Characterization of clinker and synthesized cement

213 The CaO_{free} content of the clinker measured according to the Schlafer-Bukokowski method is 1.287%, which is
 214 less than the limit value (2%). This indicates that the clinker's composition is well dosed.

215 Table 3 and Table 4 show the chemical composition of the mineral phases of the clinker identified by SEM-EDS
 216 analysis. Approximately 30 points were measured for each phase in different areas.

217 **Table 3**

218 Results of the SEM-EDS analysis on the silicate phases of the synthesized clinker.

Mineral phase	Formula	CaO/SiO ₂ (Theoretical ratio)	CaO/SiO ₂ (SEM-EDS results)
Alite	Ca ₃ SiO ₅	3	3.42
Belite	Ca ₂ SiO ₄	2	2.44

219

220 **Table 4**

221 Results of the SEM-EDS analysis on the interstitial phases of the synthesized clinker.

Mineral phase	Formula	CaO/Al ₂ O ₃ (Theoretical ratio)	CaO/Al ₂ O ₃ (SEM-EDS results)
Tricalcium aluminate	Ca ₃ Al ₂ O ₆	1.5	2.44
Calcium aluminoferrite	Ca ₄ Al ₂ O ₁₀ Fe ₂	2	2.575

222 The results of SEM-EDS analysis showed that the ratio of the main oxides in the four phases was higher than the
 223 theoretical value. A similar result was found in Gineys's et al. research on clinker synthesized in the laboratory [23].
 224 The difference between the theoretical and experimental values could be due to the presence of minor elements in
 225 the mineral phases, for example, Al and Fe in the C₃S and C₂S phases. This could influence the ratio of major
 226 elements in these phases. Table 5 show the physical characteristics of OPC 97TM cement. The Blaine surface of the
 227 cement reaches 3800 cm²/g, which respects the values of the Blaine surface targeted between 3500 and 4500 cm²/g.

228 **Table 5**
 229 Physical characteristics of OPC 97TM cement synthesized in the laboratory.

Cement	Density (g/cm ³)	Blaine surface (cm ² /g)	BET surface (m ² /g)	d10 (μm)	d90 (μm)
OPC 97TM	3.15	3800	1.224	0.72	43.31

230 The chemical composition of OPC 97TM cement is also presented in Table 6.

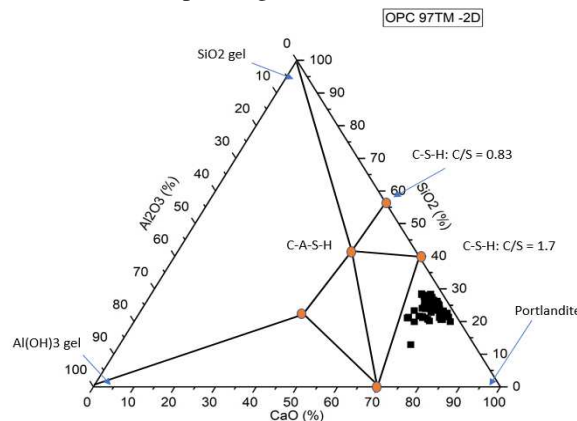
231 **Table 6**
 232 Chemical composition of OPC 97TM cement.

Element	SiO ₂	Al ₂ O ₃	Fe ₂ O ₃	CaO	SO ₃	LOI at 950 °C	Total
(wt.%)	20.5	4.7	3.1	65.5	1.90	3.6	99.2

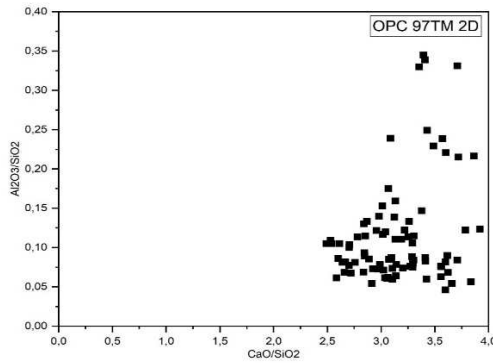
233 The chemical composition of the main elements of the hydrated calcium silicate by the SEM-EDS analysis
 234 measured on the sample of the hydrated cement paste at 2 days is presented in the Fig.1. Around 100 points were
 235 measured in four different areas. The CaO-SiO₂-Al₂O₃ ternary diagram is superimposed on the ternary diagram
 236 produced by Lothenbach [31]. This diagram shows the positions of the main cement hydrates: Ca(OH)₂, C-S-H
 237 (with two C/S ratios) or even C-A-S-H. The diagrams show that the hydrated calcium silicates are mainly
 238 concentrated in areas where the C/S ratio is greater than 1.7. A similar results have been found in previous studies
 239 on CEM I [11, 32]. Fig.2 illustrates the C/S and Al₂O₃/SiO₂ ratios of the different measured points.

240 The result show that:

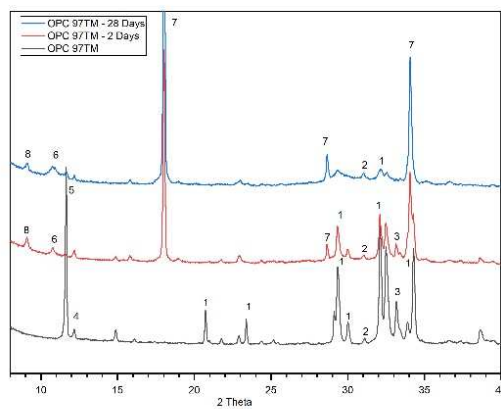
- 241 • The C/S ratio (CaO/SiO₂) obtained in the C-S-H phase varies from 2.5 to 3.5 but is always higher
 242 than the value of 1.7 used in the equations for the description of cement hydration (Eq1), (Eq2). This
 243 difference can be due to the EDS points made and to the size of the diffusion bulb which analyzes
 244 an area and not a point. Typically, the diffusion bulb's size is 1 μm³ and the resolution of a SEM 20
 245 kV tungsten filament is 3 nm. Thus, other hydrates are analyzed and will have an influence on the
 246 C/S and Al₂O₃/SiO₂ ratios, in particular, the C/S ratio [32].
- 247 • The average value of the Al₂O₃/SiO₂ ratio of hydrates measured is equal to 0.14 and this value is
 248 very consistent with the initial value of the Al₂O₃/SiO₂ ratio in the anhydrous OPC 97TM cement
 249 (the Al₂O₃/SiO₂ ratio in the cement is equal to 0.137). This result means that all of the aluminum in
 250 the cement is found in the C-A-S-H and C-S-H phases. The incorporation of aluminum into the C-S-
 251 H phase has been demonstrated in research by Richardson et al [33]. This study showed an Al/Si
 252 ratio equal to 0.25, corresponding to the maximum aluminum that can be incorporated into C-S-H.



253
 254 **Fig. 1** CaO-SiO₂-Al₂O₃ ternary diagram obtained for the cement paste after 2 days of hydration.



255
 256 **Fig. 2** Ratio of the principal elements of hydrated calcium silicate measured by SEM-EDS analysis on the sample of
 257 the cement paste after 2 days of hydration.
 258 The evolution of the mineral phases over time of hydration identified by the XRD analysis is presented in Fig.3.



259
 260 **Fig. 3** X-Ray diffraction of OPC 97TM over time of hydration (1: C₃S, 2: C₂S, 3: C₃A, 4: C₄AF, 5: Gypsum, 6:
 261 Afm, 7: Ca(OH)₂, 8: Ettringite (Aft).

262 The formation of additional phases such as ettringite and portlandite in the hydrated cement paste has been
 263 observed. These hydrates formed correspond to the products described in equations (Eq 1) -> (Eq 8). However, the
 264 presence of hydrated calcium silicate (C-S-H) is difficult to detect due to its amorphous nature.

265 The compressive strength of the cement paste is presented in the Table 7. This result is consistent with the
 266 previous XRD result showing the transformation of anhydrous phases to hydrates in hydrated cement paste, which is
 267 the origin of resistance development.

268 **Table 7**
 269 Compressive strength of the cement paste over the time of hydration.

Time (days)	Compressive strength (Mpa)	Deviation (%)
2 days	25.26	6.5
15 days	57.98	9.5
28 days	66.61	8.5

270 **III.2. Degree of hydration of cement by portlandite quantification analysis by TGA analysis**

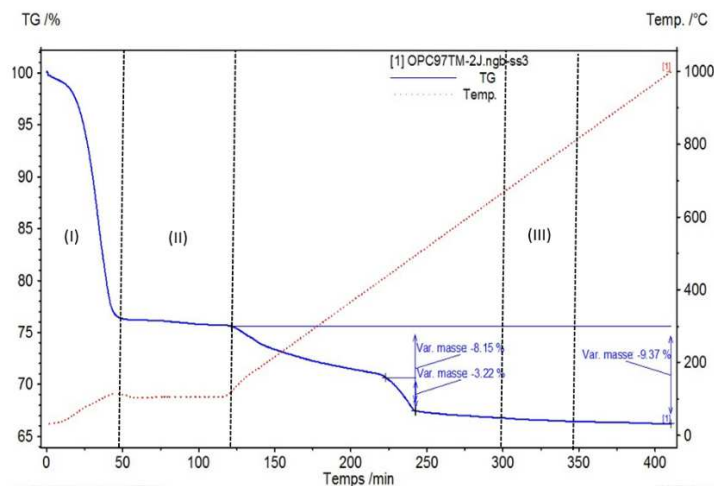
271 The amount of portlandite produced during cement hydration was estimated by TGA analysis on cement pastes
 272 at 2 and 28 days of hydration. Table 8 shows the mineral composition of the cement and the Ca(OH)₂ amount
 273 produced during complete hydration, according to the calculation from the simplified equations (Eq1) -> (Eq8).
 274 Indeed, the results of the SEM-EDS analysis on the clinker and the cement paste showed a different element ratio
 275 than the theoretical ratios used in these equations.

276 **Table 8**
 277 Ca(OH)₂ production for a complete hydration of cement of OPC 97TM cement.

Anhydrous phases	Mass content in cement (%)	CH mass for 1 g of anhydrous cement (g/g of cement)
C ₃ S	73.96	0.312
C ₂ S	4.77	0.0062
C ₃ A	5.93	0
C ₄ AF	9.77	0.0147
CaO _{free}	1.24	0
Gypsum	4.33	0
Total	100	0.3329

278 Fig.4 shows the TGA analysis curve of the cement paste after 2 days of hydration.

- 279
- 280
- 281
- 282
- 283
- 284
- Zone (I): the temperature increases from 30 °C to 105 °C to remove evaporable water.
 - Zone (II): the temperature is maintained at 105 °C for 1 hour to remove the rest of evaporable water.
 - Zone (III): the temperature between 650 °C and 800 °C corresponds to the decomposition of calcite temperature. In this case, the loss of weight of the sample is very low, this means that the protocol allows avoiding the phenomenon of carbonation and the quantity of Ca(OH)₂ determined between 450 °C and 560 °C is the totality of the Ca(OH)₂ produced during the hydration of the cement.



285

286 **Fig. 4** TGA analysis of the cement paste (w/c = 0.5) after 2 days of hydration.

287 Table 9 shows the amount of portlandite as well as the degree of hydration calculated according to (Eq10),

288 (Eq11) and (Eq12) taking the value Υ_0 (total amount of Portlandite produced when the hydration is completed)

289 equal to 0.3329 (Table 8).

290 **Table 9**

291 Quantity of Ca(OH)₂ and the degree of hydration of the cement paste over the time of hydration.

Time (days)	Portlandite mass (g/100 g of pastes)	Degree of hydration (%)
2 days	13.24	60.09
28 days	20.44	92.16

292 **III.3. Degree of hydration of cement by quantification of chemically bound water by TGA analysis**

293 This approach determines the degree of hydration of the cement according to (Eq13) and (Eq14) using TGA

294 analysis. The $W_n(\infty)$ value is calculated based on a theoretical approximation of the amount of chemically bound

295 water for the five main phases of cement upon complete hydration. Table 10 shows the theoretical amount of water

296 in the cement for complete hydration.

297 **Table 10**
 298 Theoretical amount of water bound for complete hydration of OPC 97TM cement.

Anhydrous phases	Masse content in cement (wt.%)	Quantity of bound water produced in g of water/g of phase in the cement	Mass of water related to complete hydration (g)
C ₃ S	73.96	0.24	17.75
C ₂ S	4.77	0.21	1.00
C ₃ A	5.93	0.40	2.372
C ₄ AF	9.77	0.37	3.614
CaO _{free}	1.24	0.33	0.409
Gypsum	4.33	0	0
Total	100		25.145

299 From Table 10, we conclude that the $W_n(\infty) = 25.145$ (g).

300 From the result of the TGA analysis (Fig.4), we then obtain:

301 $\Delta m_{sample} (105^\circ C - 1000^\circ C)(2\ days) = 9.37$ (g).

302 $m_{sample} (1000^\circ C)(2\ days) = 66.21$ (g).

303
$$w_n(2\ days) = \frac{\Delta m_{sample} (105^\circ C - 1000^\circ C)(t)}{m_{sample} (1000^\circ C)(t)} * 100 = \frac{9.37}{66.21} * 100 = 14.152$$
 (g).

304 The degree of hydration of the cement within 2 days of hydration was calculated using (Eq13):

305
$$\alpha(t) = \frac{W_n(t)}{W_n(\infty)} = \frac{14.152}{25.145} * 100 = 56.28$$
 (%).

306 Table 11 shows the degree of hydration of the cement paste calculated according to the method of
 307 quantification of water bound over time of hydration.

308 **Table 11**
 309 Degree of hydration of OPC 97TM cement estimated by the bound water quantification method.

Time (days)	Degree of hydration (%)
2 days	56.28
28 days	80.85

310 **III.4. Degree of hydration of cement by SEM-BSE image analysis method**

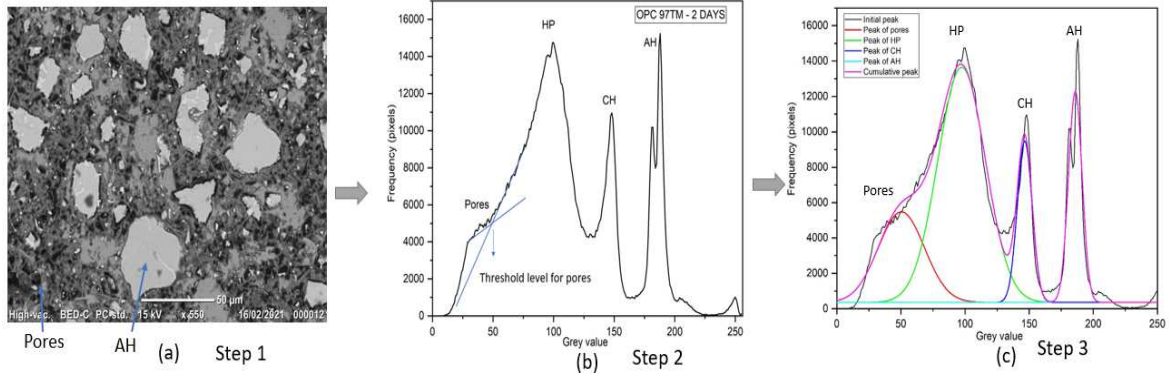
311 Fig.5 shows the essential steps applied in this study to quantify the cement phases over time of hydration.

- 312
- 313 • Step 1: Acquisition of SEM-BSE images of the sample.
 - 314 • Step 2: Acquisition of histogram of SEM-BSE images of the sample using Matlab software.
 - 315 • Step 3: Quantification of phases on the diagram of histogram using Origin pro software.

316 The segmentation of the pores from an image with gray levels (0-255), first requires the setting of a threshold
 317 value [34]. In the literature, many methods exist for determining this threshold value, which is very important for
 318 quantification with better precision, for example it corresponds to the point of intersection of the tangents to the
 319 peak curves of the pores and of the peaks of the hydrated phases (HP) (Fig.5). This threshold level of pore
 320 segmentation is around 50 for the cement paste in this study. After setting the threshold level, the deconvolution
 321 method was applied using the Origin Pro 8.5 software for phase quantification. The quantity of phases from the
 322 analysis of the images corresponds to the volume fraction of these phases in the cement paste and the degree of
 hydration of the cement is estimated according to the following equation (Eq18):

$$\alpha(t) = \frac{V_{anhydrous\ cement}(t)}{V_{anhydrous\ cement}(t=0)} * 100 \quad (18)$$

323 The cement paste made with a W/C ratio equal to 0.5 corresponds to an initial volume fraction of the cement
 324 equal to 38.83%.



325
326 **Fig. 5** Methodology of phase quantification using image analysis technique (cement paste after 2 days of hydration)

327 Several images were analyzed and the Table 12 shows the result of the degree of hydration of the cement over
328 time of hydration by the method of SEM – BSE image analysis.

329 **Table 12**
330 Degree of hydration of cement estimated by the SEM – BSE image analysis method.

Time (days)	Amount of anhydrous cement (%)	Degree of hydration (%)	Deviation (%)
2 days	14.35	63.04	7.80
28 days	2.46	93.66	8.40

331 **III.5. Assessment of the relevance of method for determining the degree of hydration**

332 Table 13 shows the degree of the OPC 97TM cement paste determined by three different methods.

333 **Table 13**
334 Degree of hydration of the OPC 97TM cement paste determined by three different methods.

Method	Degree of hydration (%)	
	2 Days	28 Days
Method 1	60.09	92.16
Method 2	56.28	80.85
Method 3	63.04	93.66

335 The deviation of the degree of hydration estimated by different methods was observed. In order to assess the
336 relevance of these methods, the Power's approach (Eq19) was used [35] which presents a model for estimating
337 compressive strength as a function of the degree of hydration.

$$\sigma_c(t) = \sigma_0(X(t))^n \quad (19)$$

338 with:

339 $\sigma_c(t)$: Compressive strength at time t.

340 σ_0 : Compressive strength when capillary porosity is zero. It is calibrated on the basis of determination of resistance
341 at 2 days.

342 n: Value taken between 2.6 and 3.0. In general, a value equal to 2.6 is applied for CEM I.

343 X(t): Ratio of hydrate gel-space, is determined as following equation (Eq20):

$$X(t) = \frac{0.68 \alpha(t)}{0.32 \alpha(t) + \frac{W}{C}} \quad (20)$$

344 with:

345 $\alpha(t)$: Degree of hydration of sample at time t.

346 W/C: water/cement ratio.

347 From the relationship between the compressive strength and the degree of hydration (Eq19) and (Eq20), the
348 experimental value of the compressive strength was used to assess the suitability of the three methods. The principle
349 is to determine the degree of hydration at 28 days from the hydration at 2 days in order to achieve desired
350 compressive strength. The degree of hydration at 28 days is calculated using the following equation (Eq21):

$$\alpha(28 \text{ days}) = \frac{0.5}{\left(\frac{0.32\alpha(2\text{days})/100+0.5}{\alpha(2 \text{ days})/100}\right)^{2.6} \sqrt{\frac{\sigma_c(2 \text{ days})}{\sigma_c(28 \text{ days})}} - 0.32)} \quad (21)$$

351 with:

352 σ_c (2 days): Compressive strength at 2 days (Mpa).

353 σ_c (28 days): Compressive strength at 28 days (Mpa).

354 α (2 days): Degree of hydration at 2 days (%).

355 α (28 days): Degree of hydration at 28 days calculated from the degree of hydration at 2 days to reach the desired
356 resistance value at 28 days (%).

357 Table 14 shows the value of the degree of hydration calculated according to (Eq21) from the degree of hydration at
358 2 days determined according to the three methods.

359 **Table 14**

360 Degree of hydration at 28 days calculated from (Eq21) according to three methods, Method 1: Portlandite
361 quantification method, Method 2: Bound water of quantification method, Method 3: SEM-BSE image analysis
362 method.

Degree of hydration	Method 1	Method 2	Method 3
α (28 days) (%) (Eq21)	102.9	97.6	111.9
α (28 days) (%) (Experimental)	92.16	80.85	93.66
Deviation (%)	11.65	20.71	19.47

363 The result shows that:

- 364 • Ca(OH)_2 quantification method seems to give a better result compared to two other methods with the
365 smallest deviation. However, the degree of hydration at 28 days calculated from method 1 and method 3
366 exceeds 100%. In addition, Zhang et al [36] found that the degree of hydration of CEM I cement paste
367 varies between 55 and 80 % at 28 days depending on the W/C ration (W/C ration between 0.3 and 0.7).
- 368 • Comparing with Zhang's result, method 2 seems to present a reasonable result. However, it should be noted
369 that some phases (Ettringite, C-S-H) start dehydroxylation at a lower temperature than 105 °C [11].

370 In addition, we chose to compare the experimental quantities of Ca(OH)_2 to evaluate the methods' relevance in
371 our study because Ca(OH)_2 is a relatively easy data set to determine thanks to TGA analysis. The SEM-BSE image
372 analysis presents the volume of Ca(OH)_2 over time of hydration. We convert from volume fraction to mass fraction
373 using a Ca(OH)_2 density of 2.24 (g/cm³). The Ca(OH)_2 /initial cement mass ratio measured by the SEM-BSE images
374 analysis method is calculated according to the following equation (Eq22):

$$\frac{\text{Ca(OH)}_2(t) \text{ mass}}{\text{initial cement mass}} = \frac{V \text{ Ca(OH)}_2(t)}{V \text{ anhydrous cement}(t=0)} * \frac{2.24}{3.15} * 100 \quad (22)$$

375 With:

376 $\text{Ca(OH)}_2(t)$ mass: Masse of Ca(OH)_2 at time t.

377 $V_{\text{Ca(OH)}_2}(t)$: Volume of Ca(OH)_2 at time t.

378 $V_{\text{anhydrous cement}(t=0)}$: Initial volume of anhydrous cement.

379 Ca(OH)_2 density : 2.24 g/cm³.

380 Cement density: 3.15 g/cm³ (Table 5).

381 The result of three methods is presented in the Table 15.

382 **Table 15**

383 Ca(OH)_2 /initial cement mass ratio measured by three methods.

$\frac{\text{Ca(OH)}_2(t) \text{ mass}}{\text{initial cement mass}}$ (%)	Method 1	Method 2	Method 3
2 Days	20.27	20.15	21.25
28 Days	30.68	29.03	31.18

384 The result shows that:

- 385 • Method 1 and method 3 seem to present the result consistent with method 2 by presenting a higher ration.
386 But the deviation is small.

387 IV. Conclusion

388 The objective of this study is to estimate the degree of hydration of cement synthesized in the laboratory by three
389 different approaches: method of quantification of portlandite, method of quantification of chemically bound water
390 and method of image analysis. The results showed that:

- 391 • The C/S ratio in the alite and the belite in the clinker measured by the SEM-EDS analysis are higher than
392 the theoretical ratio equal to 3 and 2 respectively. The CaO/Al₂O₃ and CaO/Fe₂O₃ ratios in C₃A and C₄AF
393 are also higher than the theoretical value of 1.5 and 2 respectively. The difference between the theoretical
394 and experimental values could be due to the presence of minor elements in the mineral phases, for example,
395 Al and Fe in the C₃S and C₂S phases. This could influence the ratio of major elements in these phases.
- 396 • The C/S ratio in the hydrated calcium silicate (C-S-H) phase measured by the SEM-EDS analysis on the
397 hydrated cement paste at 2 days is also higher than the theoretical value of 1.7 used in the equations of
398 cement hydration. This difference can be due to the EDS points made and to the size of the diffusion bulb
399 which analyzes an area and not a point. In addition, the incorporation of aluminum in this phase has been
400 detected. This could have an influence on the C/S ratio.
- 401 • The bound water quantification method seems to present a reasonable result using the Power's approach
402 and using the result in the literature.
- 403 • The Ca(OH)₂ quantification method seems to overestimate the degree of hydration. The result also depends
404 on the temperature range of Ca(OH)₂ quantification on the TGA curve.
- 405 • The SEM – BSE image analysis method presents relatively similar results with the results by the Ca(OH)₂
406 quantification method. This method demonstrates the feasibility used as a reliable method to determine the
407 degree of hydration, the amount of hydrates in a cementitious material. However, it is necessary to improve
408 the number of images and the resolution to increase the precision.

409 Declaration of competing interest:

410 The authors declare that they no known competing financial interests or personal relationships that could have
411 appeared to influence the work reported in this paper.

412 Acknowledgments:

413 The authors wish to acknowledge the SEDICIM project and the FEDER funds.

414

415 Reference

- 416 1. Nonat, A.: Chapitre2: L'hydratation des ciments- La durabilité des bétons. (2008)
- 417 2. Tang, S., Wang, Y., Geng, Z., Xu, X., Yu, W., A, H., Chen, J.: Structure, fractality, mechanics and
418 durability of calcium silicate hydrates. *Fractal Fract.* 5, (2021). <https://doi.org/10.3390/fractalfract5020047>
- 419 3. Wang, L., Guo, F., Lin, Y., Yang, H., Tang, S.W.: Comparison between the effects of phosphorous slag and
420 fly ash on the C-S-H structure, long-term hydration heat and volume deformation of cement-based materials.
421 *Constr. Build. Mater.* 250, 118807 (2020). <https://doi.org/10.1016/j.conbuildmat.2020.118807>
- 422 4. Richardson, I.G.: Nature of C-S-H in hardened cements. *Cem. Concr. Res.* 29, 1131–1147 (1999).
423 [https://doi.org/10.1016/S0008-8846\(99\)00168-4](https://doi.org/10.1016/S0008-8846(99)00168-4)
- 424 5. Escalante-Garcia, J.I., Sharp, J.H.: Variation in the composition of C-S-H gel in portland cement pastes
425 cured at various temperatures. *J. Am. Ceram. Soc.* 82, 3237–3241 (1999). <https://doi.org/10.1111/j.1151-2916.1999.tb02230.x>
- 426 6. Richardson, I.G.: The calcium silicate hydrates. *Cem. Concr. Res.* 38, 137–158 (2008).
427 <https://doi.org/10.1016/j.cemconres.2007.11.005>
- 428 7. Phung, Q.T., Maes, N., Jacques, D., Perko, J., De Schutter, G., Ye, G.: Modelling the evolution of
429 microstructure and transport properties of cement pastes under conditions of accelerated leaching. *Constr.*
430 *Build. Mater.* 115, 179–192 (2016). <https://doi.org/10.1016/j.conbuildmat.2016.04.049>
- 431 8. Snellings, R., Vayghan, A.G., Horckmans, L., Snellings, R., Peys, A., Teck, P., Maier, J., Friedrich, B.,
432 Klejnowska, K.: Use of Treated Non-Ferrous Metallurgical Slags as Supplementary Cementitious Materials
433 in Cementitious Mixtures Use of Treated Non - Ferrous Metallurgical Slags as Supplementary Cementitious
434 Materials in Cementitious Mixtures. (2021). <https://doi.org/10.3390/app11094028>
- 435 9. Kocaba, V., Gallucci, E., Scrivener, K.L.: Methods for determination of degree of reaction of slag in
436 blended cement pastes. *Cem. Concr. Res.* 42, 511–525 (2012).
437 <https://doi.org/10.1016/j.cemconres.2011.11.010>
- 438 10. Lu, X., Ye, Z., Wang, S., Du, P., Li, C., Cheng, X.: Study on the preparation and properties of belite-
439 ye'elimite-alite cement. *Constr. Build. Mater.* 182, 399–405 (2018).
440 <https://doi.org/10.1016/j.conbuildmat.2018.06.143>
- 441 11. Cassagnabère, F., Mouret, M., Escadeillas, G.: Early hydration of clinker-slag-metakaolin combination in
442 steam curing conditions, relation with mechanical properties. *Cem. Concr. Res.* 39, 1164–1173 (2009).
443 <https://doi.org/10.1016/j.cemconres.2009.07.023>
- 444 12. Bentz, D.P., Barrett, T., De la Varga, I., Weiss, W.J.: Relating Compressive Strength to Heat Release in
445 Mortars. *Adv. Civ. Eng. Mater.* 1, 20120002 (2012). <https://doi.org/10.1520/acem20120002>
- 446 13. Ha, B.T.T.: Evolution physico-chimique des liants bas PH hydratés Influence de la température et
447

- 448 mécanisme de rétention des alcalins - Thèse doctorante, (2010)
- 449 14. Benzerzour, M., Maherzi, W., Amar, M.A.A., Abriak, N.E., Damidot, D.: Formulation of mortars based on
450 thermally treated sediments. *J. Mater. Cycles Waste Manag.* 20, 592–603 (2018).
451 <https://doi.org/10.1007/s10163-017-0626-0>
- 452 15. Bordy, A.: Influence des conditions thermo-hydriques de conservation sur l'hydratation de matériaux
453 cimentaires à base d'une fine recyclée. 1–155 (2016)
- 454 16. Elkarim, M., Bulteel, D., Potier, G., Michel, F., Zhao, Z., Courard, L.: Use of grinded hardened cement
455 pastes as mineral addition for mortars. (2020). <https://doi.org/10.1016/j.jobe.2020.101863>
- 456 17. Bresciani, C.: Simulation numérique de l'hydratation et du développement des propriétés physiques et
457 mécaniques d'une pâte de ciment afin de sélectionner de nouveaux ajouts minéraux., (2009)
- 458 18. NIST: Technical Note VCCTL-01.
- 459 19. Wong, H.S., Head, M.K., Buenfeld, N.R.: Pore segmentation of cement-based materials from backscattered
460 electron images. *Cem. Concr. Res.* 36, 1083–1090 (2006). <https://doi.org/10.1016/j.cemconres.2005.10.006>
- 461 20. P.J. Goodhew, J. Humphreys, R.B.: *Electron Microscopy and Analysis*, 3rd edition. aylor Fr. London, 2001,
462 251 pp. (2001)
- 463 21. Scrivener, K.L., Patel, H.H., Pratt, P.L., And, Parrott, L.J.: Analysis of Phases in Cement Paste using
464 Backscattered Electron Images, Methanol Adsorption and Thermogravimetric Analysis.
- 465 22. LE, T.: Influence de l'humidité des granulats de béton recyclé sur le comportement à l'état frais et durcissant
466 des mortiers, (2015)
- 467 23. Gineys, N.: Influence de la teneur en éléments métalliques sur les propriétés techniques et
468 environnementales du ciment Portland, (2011)
- 469 24. Bogue, R.H., Lerch, W.: Hydration of Portland Cement Compounds. *Ind. Eng. Chem.* 26, 837–847 (1934).
470 <https://doi.org/10.1021/ie50296a007>
- 471 25. Association Française de Normalisation (AFNOR): NF EN 196-6 : Méthodes d'essai des ciments -
472 Détermination de la finesse. (2018)
- 473 26. Aouad, G., Laboudigue, A., Gineys, N., Abriak, N.E.: Dredged sediments used as novel supply of raw
474 material to produce Portland cement clinker. *Cem. Concr. Compos.* 34, 788–793 (2012).
475 <https://doi.org/10.1016/j.cemconcomp.2012.02.008>
- 476 27. Joelle Kleib: Ecoconception des ciments : synthèse , hydratation et durabilité-Thèse doctorant IMT Lille
477 Douai et L'Université Libanaise, (2018)
- 478 28. Kleib, J., Aouad, G., Abriak, N.E., Benzerzour, M.: Production of Portland cement clinker from French
479 Municipal Solid Waste Incineration Bottom Ash. *Case Stud. Constr. Mater.* 15, e00629 (2021).
480 <https://doi.org/10.1016/j.cscm.2021.e00629>
- 481 29. Kleib, J., Aouad, G., Khalil, N., Zakhour, M.: Incorporation of zinc in calcium sulfoaluminate cement
482 clinker. *Adv. Cem. Res.* 1–7 (2020). <https://doi.org/10.1680/jadcr.19.00125>
- 483 30. Zhang, J., Scherer, G.W.: Comparison of methods for arresting hydration of cement. *Cem. Concr. Res.* 41,
484 1024–1036 (2011). <https://doi.org/10.1016/j.cemconres.2011.06.003>
- 485 31. Lothenbach, B., Scrivener, K., Hooton, R.D.: Supplementary cementitious materials. *Cem. Concr. Res.* 41,
486 1244–1256 (2011). <https://doi.org/10.1016/j.cemconres.2010.12.001>
- 487 32. Berthomier, M.: Etude de la lixiviation de l'aluminium de matériaux cimentaires à base de CEM III utilisés
488 dans les canalisations d'eau potable : approche expérimentale et numérique. (2020)
- 489 33. Richardson, I. G. A. R. Brough, et al: Location of Aluminum in substituted calcium silicate hydrate, C-S-H,
490 gels as determined by ²⁹Si and ²⁷Al NMR and EELS. 1993.
- 491 34. Zined, B.: Influence de la microstructure sur le transport diffusif des pâtes, mortiers et bétons à base de
492 CEM I avec ajout de fumée de silice, (2016)
- 493 35. Bentz, D.P.: *Guide to Using CEMHYD3D: A Three-Dimensional Cement Hydration and Microstructure
494 Development Modelling Package.* (1997)
- 495 36. Zhang, S., Zhang, M.: Hydration of cement and pore structure of concrete cured in tropical environment.
496 *Cem. Concr. Res.* 36, 1947–1953 (2006). <https://doi.org/10.1016/j.cemconres.2004.11.006>
497